Check for updates

Synthesis of ppy–MgO–CNT nanocomposites for multifunctional applications†

K. Bharathi Yazhini, [iD] Xin Wang, [iD] Qixing Zhou* and Brim Ondon Stevy

Cotton is one of the most important raw materials for textile and clothing production. The main drawbacks of cotton fibers are their poor mechanical properties and high flammability. Compared with some synthetic polymer fibers, cotton fabrics treated with modern flame-retardant and reinforcement finishes often cannot meet rigid military specifications. Polypyrrole–magnesium oxide (ppy–MgO) and polypyrrole–magnesium oxide–carbon nanotube (ppy–MgO–CNT) composites were prepared with various weight ratios by *in situ* chemical polymerization method. 1,2,3,4-Butane tetracarboxylic acid (BTCA) was used as a cross-linking agent in the presence of sodium hypophosphite (SHP). The composite sol was coated on cotton fabric using the pad-dry-cure technique. The coated cotton fabrics were characterized by SEM, EDAX, XRD, UV-DRS and FT-IR analysis, and tested for flame retardant and UPF application. The flame-retardant study showed a maximum char length of 0.3 cm and the char yield was about 49% for the ppy–MgO–CNT composite. For that UPF application, a 30 UPF value was shown for the ppy–MgO–CNT composite. In the case of the antibacterial study, the zone of inhibition was observed for all of the test samples against MRSA and PAO1 bacteria. The zone of inhibition showed as 4.0, 3.0 mm for the ppy–MgO–CNT composite. Hence, the ppy–MgO–CNT composite was found to be efficient.

1. Introduction

Over the past few decades, the modification of textiles has attracted much attention due to its increasing awareness of human beings toward environmental protection, as well as for a safe, healthy and comfortable life.[1–3] Multifunctional textiles can be fabricated through combined treatments using several materials with a specific property of fibers.[4] Cellulose is the most abundant biopolymer found on Earth and has many excellent qualities, such as biodegradability, biocompatibility, and eco-friendliness.[5] Textile industries have been focusing on improving its functional properties, such as fire retardancy, UV protection, self-cleaning and antibacterial properties. High-performance textile materials are greatly appreciated by more discerning and demanding consumer markets. Nanoparticles of metal oxides have been used to incorporate functional properties into textiles. Attempts have been made to use common metal oxides, such as titanium oxide (TiO_2), zinc oxide (ZnO), cupric oxide (CuO) and magnesium oxide (MgO), for providing fabrics with functional properties.[6] Magnesium oxide (MgO) nanopowder is a non-toxic white powder widely used in industrial applications, such as ceramics, electronics, catalysis, paints and oils. It is one of the most useful refectory materials

that improve textile functionalities, such as fire retardancy, UV protection and antibacterial properties, with toxic waste remediation.[7–10] The application of nanotechnologies benefits the textile industry by enabling the creation of new fabrics with enhanced and multifunctional material properties.[11–13] A new approach of nanomaterials has attracted researchers by worldwide finishers of textile materials. For example, nanoparticles of metal (Ag, Au, and graphene) and metal oxides (such as TiO_2, MgO, SiO_2, CuO, ZrO_2 and ZnO) have been used to functionalize textile fabrics by cotton using various approaches. The incorporation of nanoparticles in such fabric materials improves their functional features, such as UV protection, antibacterial activity, flame retardancy, thermal stability, and physicochemical properties.[14] In recent years, the use of a nano titanium dioxide photo-catalyst to cover textiles and the improvement of its surface have expanded due to its ability to absorb ultra-violet irradiation. In addition, the coat of nano TiO_2 particles on fabrics will not affect their breathability and texture.[15–23] The size and surface area of NPs may be responsible for their toxicity, but most of the studies do not reveal the relationship between the physiochemical characteristics of NPs and their toxicity.[24] For example, 25 nm anatase and 31 nm anatase/rutile show greater phototoxicity than 142 nm anatase and 214 nm rutile NPs.[25] All the sizes and crystal forms (anatase and rutile) of TiO_2 NPs exert toxic (phototoxic) effects on human skin keratinocytes under UVA irradiation in a dose-dependent way. The smaller size nTiO2 may cause greater cytotoxicity than larger size NPs, and the anatase form may show more

Key Laboratory of Pollution Processes and Environmental Criteria (Ministry of Education), College of Environmental Science and Engineering, Nankai University, Tianjin 300071, China. E-mail: Zhouqx@nankai.edu.en

phototoxicity than rutile.[26] Furthermore, the NPs (rod and sphere) of smaller size show higher toxicity than larger particles. Moreover, the nanorods exhibit more toxicity than spherical particles having the same size and surface area, showing the contribution of shape toward cytotoxicity.[27] Several methods can be used to apply finishing materials onto fabrics, such as, spraying, transfer printing, foaming, and padding, among which padding is the most commonly used method. At the same time, various polycarboxylic acids were investigated[28–33] as cross-linkers for the durable press finishing of cotton. The formaldehyde-free formation of ester linkages that improve the tensile and abrasion strength is among the advantages of these compounds.[34–36] Polycarboxylic acids, such as citric acid (CA) and 1,2,3,4-butane tetra carboxylic acid (BTCA), are cotton cross-linking agents.[37–41] These are environment-friendly and can be a suitable substitute for methylals, which contain cross-linkers. Cross-linking of BTCA and CA with cotton fabrics has been proposed to be catalyzed by sodium hypophosphite in acidic conditions. The mechanism of cross-linking is suggested to include cyclic anhydrides as reactive intermediates, which are trapped by hydroxyl groups of fabrics.[42]

Other oxygen-containing compounds like phosphates or carbonates, as well as noble metal nanoparticles, can be produced in the appropriate flame environment.[43,44] As one of

subsequently used to coat cotton fabrics using the pad-dry-cure method for multifunctional applications.

2. Experimental

2.1. Materials and methods

Woven cotton fabric of 80 counts was obtained from South Indian Textile Research Association (SITRA), Coimbatore. The pre-treatment was carried out for the grey fabric by one pot method. The recipe used was 0.4 ml hydrochloric acid (HCl), 39 g sodium carbonate (Na_2CO_3), 1.9 g sodium hydroxide (NaOH) and 1.9 ml hydrogen peroxide (H_2O_2) taken in a 300 ml beaker containing 200 ml of water. Grey cotton fabric (8 cm × 4 cm) was immersed in the bath at 80 °C for 90 min. Magnesium oxide nanoparticles (MgO) (Sigma Aldrich, 97%) with an average size of 50 nm, pyrrole (ppy) (Sigma Aldrich, 99% pure), 1,2,3,4-butane tetracarboxylic acid (BTCA) (Alfa Aesar, 98%), ammonium persulfate (APS) (Alfa Aesar, 98%), single wall carbon nanotube (CNT) (Sigma Aldrich, 97%) with an average size of 25 nm, sodium hypophosphites (SHP) (S.D. Fine, 98%), and polyethylene glycol (Alfa Aesar, 98%) were purchased and used.

2.2. Synthesis of polypyrrole
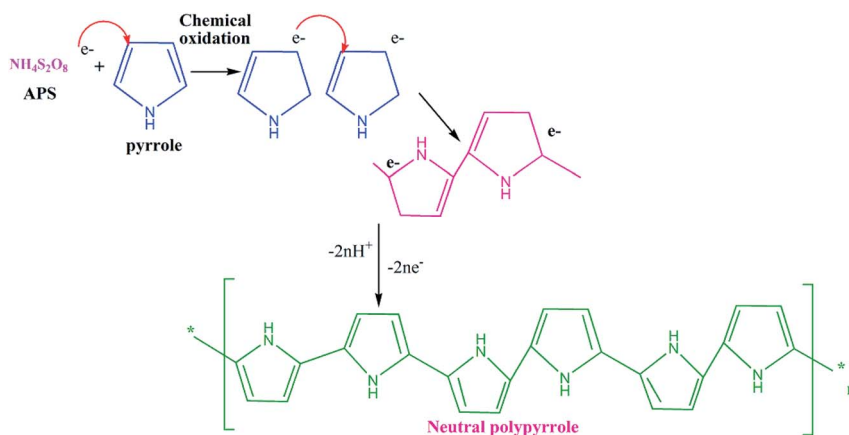
the most significant conducting polymers, ppy has been widely used in electronic devices, biomedical devices, sensors, and other fields for its good conductivity, thermal and photostability in air.[45] Since ppy also tends to swell and shrink in cycling, many ppy–GO composites have been fabricated to pledge high performance when used for super capacitors.[46]

To the best of our knowledge, no detailed investigation has been carried out so far on the utility of ppy–inorganic (metal oxide) composite coatings on the fabrics flame retardancy grounds. In this work, attempts have been made with different ratios of ppy–MgO composite and ppy–MgO–CNT by *in situ* chemical polymerization method. The nanocomposites were prepared as sol, and

Pyrrole was purified by double distillation method before use. A volume of 33.6815 ml of pyrrole (0.3 M) was dissolved in 500 ml de-ionized water. After 10 min, APS of 0.1329 g (0.06 M) was prepared in 100 ml de-ionized water and added drop wise. This solution was stirred for 24 h in an ice bath at 0 °C constantly. Excess methanol was poured to regulate the reaction. A black precipitate was obtained. This precipitate was collected and washed with different solvents, such as de-ionized water, methanol and acetone. Then, the sample was dried at 30 °C for 12 h in a vacuum oven.[47] After that, it was weighed as 32.57 grams.

2.3. Synthesis of ppy–MgO and ppy–MgO–CNT composites by *in situ* polymerization

Pyrrole of (0.3 M) was dissolved in 500 ml de-ionized water. After 10 min, BTCA (0.1 M) and SHP (1 g) catalyst were added. Stirring was carried out for 30 min at room temperature. A required amount of NaOH was added to bring the pH to neutral. APS (0.06 M) was prepared in 100 ml de-ionized water. MgO (0.25 g) was mixed with the above solution. The solution was sonicated for 30 min. The resulted solution turns milky white. This milky white solution was added dropwise into the above solution, and stirring was carried out for 9 h under a cooling condition at 20 °C. This solution was allowed to settle overnight. A black precipitate was obtained. The precipitate was collected and washed with different solutions, such as de-ionized water, methanol and acetone. Then, the sample left dried at 30 °C for 6 h in a vacuum oven. The procedure has resulted in a ppy–MgO composite at 1 : 1 ratio. This procedure was again extended to prepare ppy–MgO composites at 1 : 2 and 1 : 3 ratios and optimized. In a similar ratio way, CNT at different ratios was added. The samples were designated as ppy–MgO M_1 (1 : 1), ppy–MgO M_2 (1 : 2), ppy–MgO M_3 (1 : 3) and ppy–MgO–CNT M_4 (1 : 3 : 1). The weight gain was as follows: M_1 (0.34 g), M_2 (0.38 g), M_3 (0.40 g), M_4 (0.45 g). It has been weighted. Cross-linking can be thought of as reducing the number of chain ends, and effectively increasing the molecular weight of polymer system.[48] In general, cross-linking will increase the strength of the material.[49] The ppy–MgO composite was confirmed with XRD and FT-IR peak analysis.

2.4. Coating sol preparation

The ppy–MgO or ppy–MgO–CNT composite was prepared by mixing with polyethylene glycol (2 ml). Then, 6 ml deionized water was added into 100 ml absolute ethanol and stirred vigorously at room temperature for 30 min until a homogeneous solution was obtained. Then, 4 ml ammonia was added dropwise into this solution, and was kept under ultrasonic irradiation for 30 min to form the ppy–MgO or ppy–MgO–CNT composite sol. This sol of about (10 g m^{-2}) was used for the coating of fabric using the pad-dry-cure method.[50] The dried cotton fabric was first dipped in ppy–MgO or ppy–MgO–CNT composite sol. The wetted fabric was pulled into the nip between two rotating cylinders in the padding mangle to obtain a uniform coating. This procedure was repeated three times to obtain effective deposition of nanoparticles onto the fabric surface. Afterwards, the padded fabrics were air-dried and cured at 180 °C for 5 min in a hot-air oven. The ppy–MgO or ppy–MgO–CNT nanoparticles were linked to the fabrics with an exchange reaction between the –OH groups of cotton.

3. Results and discussion

3.1. XRD analysis

Fig. 1 illustrates the XRD patterns of the pristine MgO, polypyrrole, M_1, M_2, M_3, and M_4 composite materials. The pristine polypyrrole showed a band (curve b). It has a broad band at lower diffraction angles around 26°, which indicates the amorphous nature. This broadening of the band can be ascribed to the scattering of the bare ppy chains at the interplanar spacing.[51] Pristine MgO shows intense peaks at 42.5°, 62.1°, and 75.5°, indicating the crystalline nature with cubic structure (curve a). The peaks corresponding to the planes (200), (220) and (222) are in good agreement with JCPDS file no. 04-0829.[52] M_1 and M_2 composites (curve c and d) show an amorphous nature. There is no defined diffraction peak in the composites. When the ratio of the MgO colloidal solution was increased, the peak intensity also increased accordingly. The sharp diffraction peak of MgO implies that MgO is crystalline in nature. It is indicated by the corresponding peaks to the (200), (220) and (222) planes in the (curve e). All of these peaks match very well with the standard MgO of the cubic structure (JCPDS card 04-0829). The crystallite size of ppy–MgO calculated using Scherrer's formula was found to be 18 nm.

$$L_s = \kappa\lambda/\beta_s \cos(\theta_B)$$

where κ stands for a geometrical factor that depends on the crystallite apparent radius of gyration from the perspective of reflections with Bragg angle θ_B for X-rays of wavelength λ.

For instance, crystallites with a cubic shape have κ' 0.92, while spherical crystallites have κ' 1.18.

An additional peak is shown as the (002) plane, which indicates the presence of CNT.[53] The decrease in the intensities of the MgO peaks in the ppy–MgO–CNT functionalized average size of about 50–75 nm (curve f). It is noted that the ppy–MgO and ppy–MgO–CNT nanocomposites are more crystalline in nature than pristine polypyrrole. These results also indicate that MgO and MgO–CNT nanoparticles are incorporated in the polypyrrole matrix as composites.

Ppy, M_3 and M_4 composites were optimized for further work. The composite sols were coated on cotton fabric. Fig. 2 shows the presence of MgO nanoparticles on the surface of the fabrics. The diffraction peaks observed at 42.5°, 62.1° and 75.5° are correlated with the formation of cubic MgO assigned to the (200), (220), and (222) planes (curve c). Strong, sharp diffraction
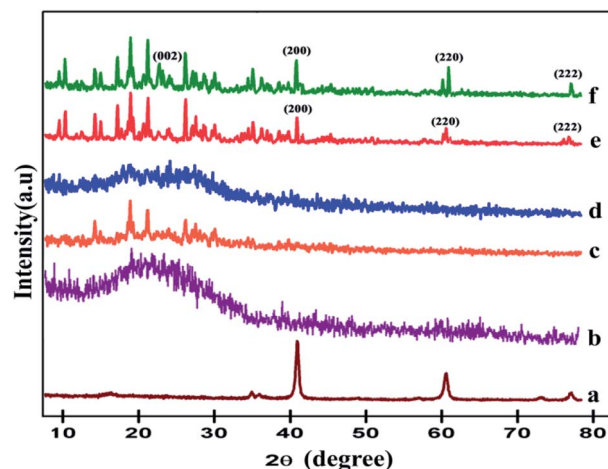

Fig. 1 XRD patterns of the pristine (a) MgO, (b) polypyrrole, (c) M_1, (d) M_2, (e) M_3, and (f) M_4 composite materials.
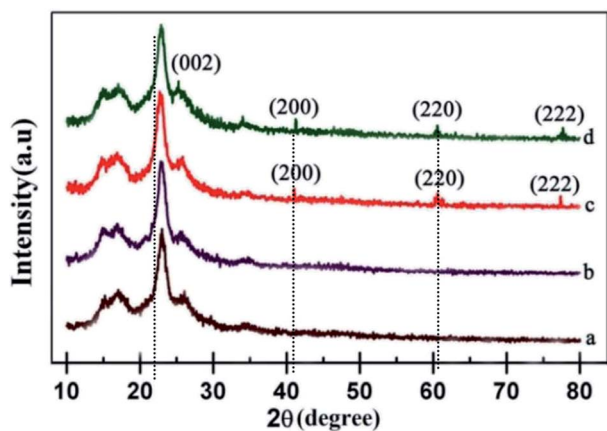
Fig. 2 XRD patterns of (a) uncoated, (b) ppy-coated, (c) M_3-coated, and (d) M_4-coated cotton.

peaks indicate that the ppy–MgO–CNT was well crystallized. An additional sharp peak is shown at the (002) plane, which indicates the presence of CNT (curve d). The equal ratio of ppy–MgO shows strong peaks. It was observed that the MgO particle interacts on the polypyrrole surface.

3.2.   FT-IR analysis

Fig. 3 shows the FTIR-ATR spectra of uncoated, ppy, ppy–MgO and ppy–MgO–CNT coated fabrics. In all coated and uncoated fabrics, the absorption peaks observed at 3300, 2899, 1679, 1426, 1240, 1157, and 1051 cm^{-1} are ascribed to –OH stretching, –CH stretching, H–O–H bending, –CH bending, C–O–C asymmetric glucose ring, and C–O stretching, respectively, for cellulose on the cotton fabrics.[54] The ppy spectrum (curve b) shows the characteristic peak attributed to the C–H in-plane deformation vibration at 1051 cm^{-1}, N–C stretching band at 1240 cm^{-1}, and C–C asymmetric stretching vibration at
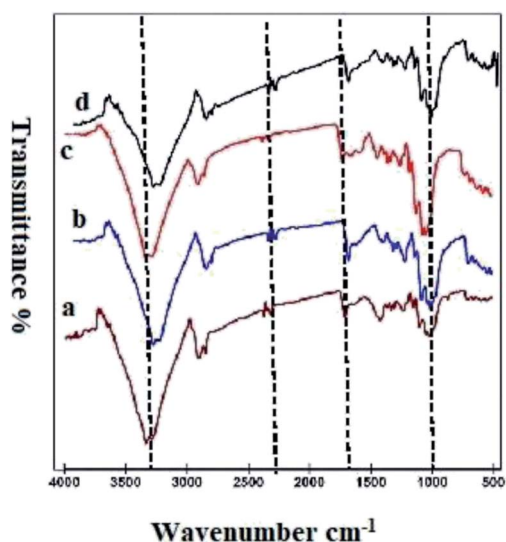
1427 cm^{-1}.[52] A peak was observed at 1697 cm^{-1} for the untreated fabric (curve a). This peak is shifted to 1716 cm^{-1}, which may be due to the cross-linking between cotton and BTCA (curves c and d). There is no structure change, just cross-linking of the cotton fabric and BTCA.[55] The hetero polar diatomic molecular vibrations of MgO were confirmed by the peak at 680 cm^{-1}.[56]

3.3.   SEM analysis

Fig. 4 shows the surface analysis of the coated and uncoated fabrics to investigate the morphological change. The MgO nanoparticles, ppy–MgO, ppy–MgO–CNT nanocomposites are grafted on the fabric surface. The uncoated fabric shows a plain surface when compared to the ppy-, M_3- and M_4-coated fabrics.

Fig. 3 FTIR-ATR spectra of (a) uncoated cotton, (b) ppy-coated, (c) M_3-coated, and (d) M_4-coated cotton.
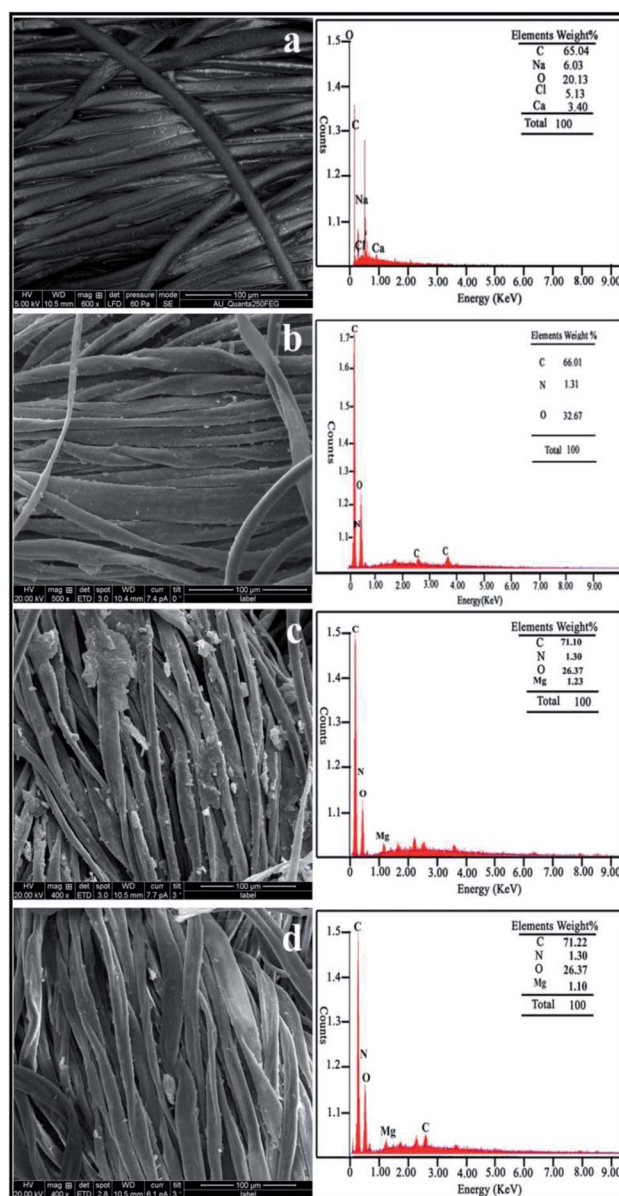

Fig. 4 FE-SEM images with EDAX micrographs of the (a) uncoated, (b) ppy-coated, (c) M_3-and (d) M_4-coated cotton fabrics.
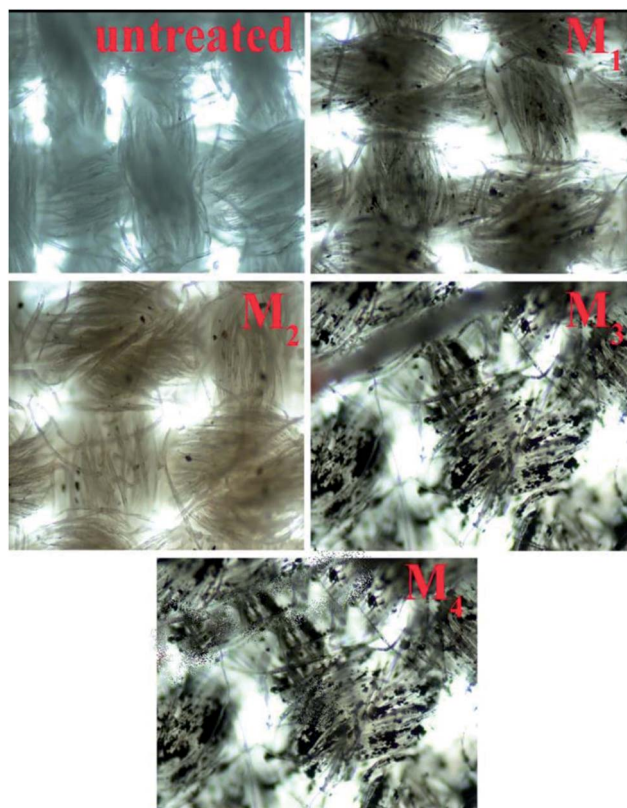
Fig. 5 Optical microscopic images of the uncoated, and M_1-M_4 coated fabrics.

Table 1 Vertical flammability test and the results

Test sample	Flammability (45 °C)	
	Char length (cm)	Char yield (%)
Untreated cotton	2.0	85
Ppy-coated cotton	1.9	65
MP_1-coated cotton	1.0	48
MP_2-coated cotton	1.4	47
MP_3-coated cotton	0.5	44
MPN-coated cotton	0.3	49

there is the presence of CNT (71.22) nanoparticles, due to the increase in carbon coating on the M_4 coated fabric. These results confirm the effective coating of the nanoparticles on the surface of the fabric.

3.4. Optical microscopic analysis

Fig. 5 shows the optical microscopic observation that the colorless uncoated fabrics were coated with composites, making them brownish in color. The surface modification of the coated fabric was confirmed by the crosslinking agents, which is present in the coated fabric.

The composite particle in the microscopic images (Fig. 5) of M_1 to M_4 show the presence of ppy–MgO composite in the coated fabric.

3.5. TGA-DTG analysis

The thermogravimetric analyses with TGA (a) and DTG (b) are shown in Fig. 6. The samples were heated up to 600 °C at a heating rate of 10 °C min^{-1} under a nitrogen flow rate of 20 ml min^{-1}. Image a summarizes the thermal degradation of the uncoated cotton and that of the coated cotton with M_3 and M_4. The TGA curves of cotton consist of three stages as the initial, main, and char decomposition regions. In the first stage, weight loss is due to some physical changes that occurred mostly in the amorphous region of the cellulose. In this stage, the mass loss

Image (b) shows the pebble-shaped MgO nanoparticles adhering to the fabric surface, whereas needle-like small agglomerated ppy–MgO nanocomposite particles are seen in image (c). The uniform coated ppy–MgO–CNT composite nanoparticles are shown in image (d). The EDAX images indicate the presence of magnesium, oxygen, and carbon in the coated fabric. From the above studies, the elemental wt% of the M_4 fabric (1.10) was found to be decreased when compared to that of the M_3 fabric (1.23) and uncoated fabric. It indicates
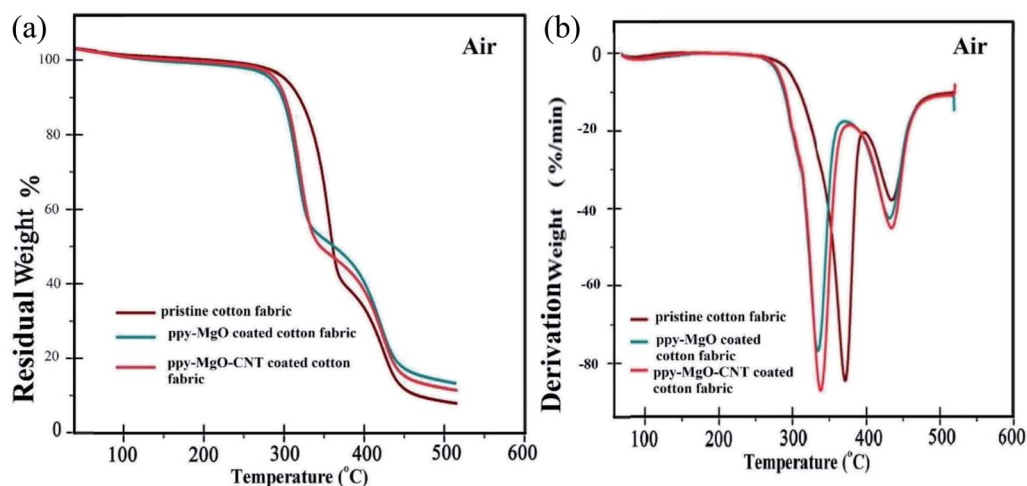

Fig. 6 TGA (a) and DTG (b) curves of the uncoated fabric, ppy–MgO composite-coated fabric, and ppy–MgO–CNT composite-coated fabric.
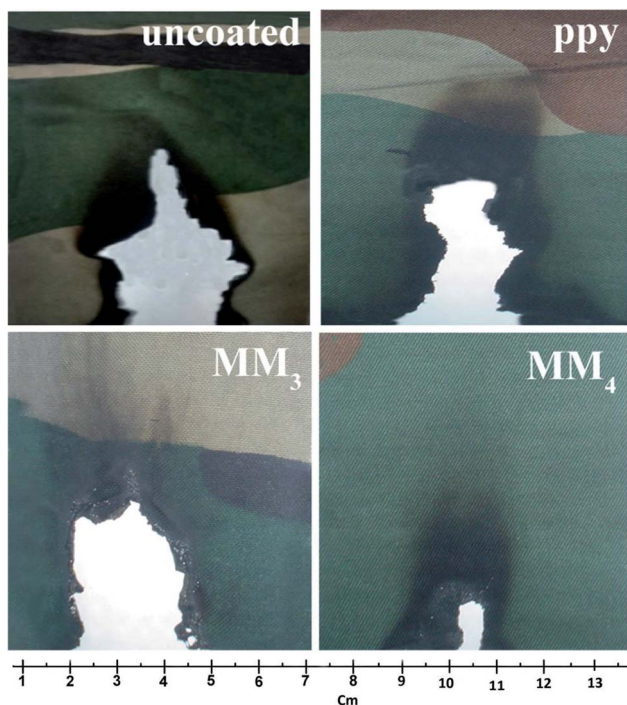
Fig. 7 Images of the vertical flame testing of the uncoated and composite-coated cotton fabrics (ppy, MM$_3$ and MM$_4$).

Fig. 9 Transmittance *versus* wavelength for differently treated samples in UV analysis: (a) uncoated cotton, (b) pyrrole coated cotton, (c) M$_1$ coated, (d) M$_2$ coated, (e) M$_3$ coated, (f) M$_4$ coated.

the CNT. The DTG curve revels that the burning step is broadened by the presence of ppy. Therefore, the associated heat of combustion is spread in a wider range of temperatures. These findings point out that ppy–MgO–CNT alters the combustion process of cellulose. The residual weight at 385 °C for all of the coated samples is more than double that of the uncoated cotton.

3.6. Evaluation for flame retardant

The combustion processes of pristine cotton fabric, ppy coated cotton fabric, M$_3$, and M$_4$ composite coated fabric were treated. The untreated cotton fabric and the composite-treated cotton samples were hung on a metal supporter, and then ignited with a lighter. The uncoated cotton caught fire immediately. With the progress of the burning, it burns to ashes completely. However, the M$_3$ and M$_4$ composite-coated cotton did not burn and just charred on the edge, forming a stiff sinter (transfer of CNTs). These results provide direct evidence of the flame-retardant effect of CNT on cotton textiles. The results of the vertical flammability test are summarized in Table 1. The results depict that the coatings decreased the flammability of the test samples. Noticeably, the BTCA cross-linked with ppy–MgO and ppy–MgO–CNT composite-coated cotton fabrics were

between 50 °C and 205 °C is due to the loss of water and unreacted substances. In the second stage, the weight loss between 205 °C and 440 °C indicated the decomposition of polymer chains. It is stated by different researchers that glucose together with combustible gases are generated in this stage.[57] It is reported that thermal degradation in this stage takes place in the crystalline region of the cellulose fibers. The formation of char occurs in the third stage at the higher temperature of 500 °C. This could be due to de-watering and charring reactions, releasing water and carbon dioxide, and increasing charred residues.[58,59] The test sample cross-linked with CNT and BTCA showed superior degradation temperature in the second region. This improvement of thermal properties is attributed to the high heat resistance, the heat insulation effect, and the mass transport barrier toward cellulose molecular chains exerted by
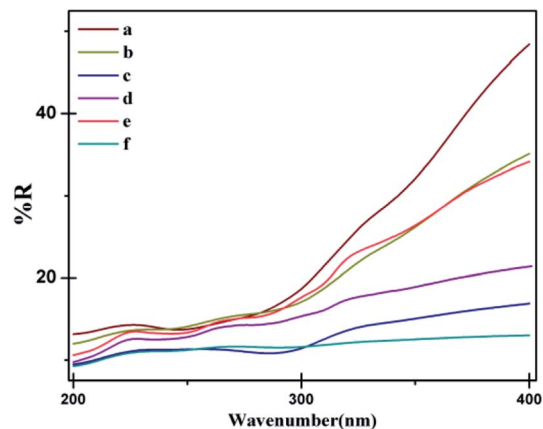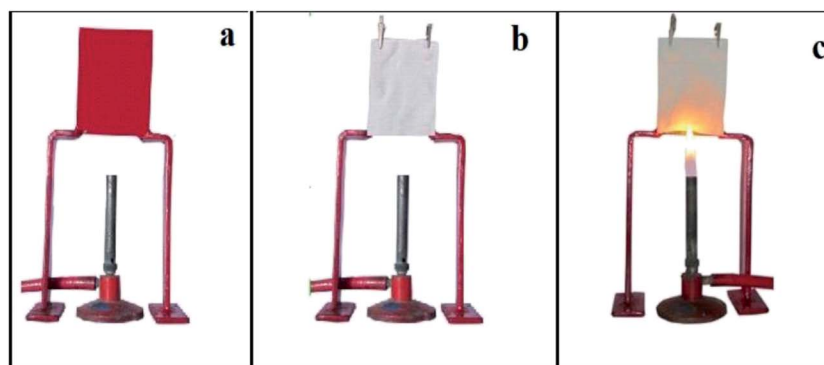

Fig. 8 (a) Indigenously developed apparatus for flammability test. (b) Fabric sample mounted on the test area. (c) Fabric under flammability test.

Table 2 Effect of ratios of ppy–MgO and ppy–MgO–CNT composites coated on cotton for UV protection of uncoated and composite coated cotton fabrics

Composition	UPF value	UV protection
Uncoated cotton	6	Not considerable
Ppy coated cotton	13	Not considerable
M_1 coated cotton	16	Good
M_2 coated cotton	20	Good
M_3 coated cotton	25	Good
M_4 coated cotton	30	Good

Table 3 Antibacterial test results of the composite coated fabrics

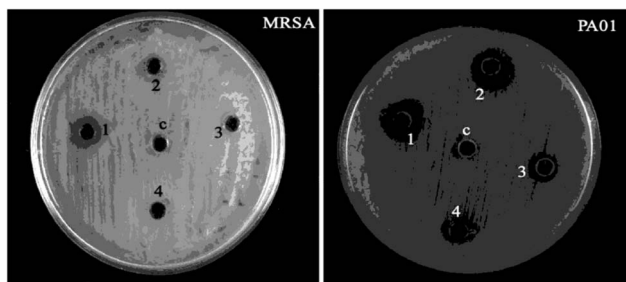| Test sample	Zone of inhibition (mm)	
	MRSA	PAO1
M_1 composite	1.0	1.0
M_2 composite	2.1	1.5
M_3 composite	3.1	2.1
M_4 composite	4.0	3.0

Fig. 10 Antibacterial activity (negative control) of © DMSO, (1) M_1, (2) M_2, (3) M_3 and (4) M_4.

effective in reducing flammability. The M_3 and M_4 composite-coated fabrics showed decreased char length and increased char yield. These results confirmed the effect of impregnation of phosphorus on the coated fabric. M_4 shows low char yield compared to other fabrics due to the effective and uniform deposition of the composite. Flame-retardant and super paramagnetic zinc ferrite (ZF) was adopted to decorate boron nitride nanosheet (BNNS) through a typical solvothermal method, so as to afford a ZF-BNNS nanofiller with improved flame-retardant performance. As a result, the density and strength of the carbon layers are increased in association with enhanced insulation shield effect to heat flux, oxygen and combustible pyrolysis products, as well as their suppression to release and transfer during combustion.[60]

The optimized composite sol of M_3 and M_4 were applied to military uniforms and designated as MM_3 and MM_4, respectively. The uncoated fabric showed a char length of 7.5 cm and char yield of 72%. The MM_3-coated fabric shows a char length of 3.2 cm and char yield of 75%. The MM_4-coated fabric shows a char length of 2.1 cm and char yield of 87% (Fig. 7).

The size of the specimen should be to 8 cm × 10 cm.

If the specimen has a raised fiber surface, it has to be prepared by brushing.

If the specimen has a flame-retardant finish, then it has to be prepared by dry-cleaning, laundering and drying.

The dried specimen of the fabric is to be fixed on the side of the test area.

Standardized flame is to be applied to the fabric surface near the lower end.

The time required for the flame to proceed up the fabric a distance of 127 mm is measured as showed in Fig. 8.

Char yield is noted.

Char length is noted.

The burnt sample length is measured with a scale as the char length in cm value. The measurement of the char yield is an appropriate element in determining the flame retardancy.[61] The weight of each sample before and after burning is measured, and the char yield is calculated as $[W_2/W_1] \times 100$, where W_1 and W_2 are the weight of the sample before and after burning.

Table 1 shows that the coatings decreased the flammability of the samples. These results confirmed the impact of phosphorus deposited from SHP. Evidently, BTCA crosslinked with ppy–MgO and ppy–MgO–CNT composite-coated fabrics are effective in reducing flammability of treated fabrics in the presence of SHP. The char length of the samples was measured in the vertical flammability test, and the results are reported in Table 1. The differences in the burning behavior and char length in the vertical flame test between the uncoated sample and composite coated fabrics are the indicators of the flame retardancy and effect. It is noted that the increase of the MgO and CNT ratios has led to a decrease in the fabric flammability. It is interesting to observed that the charred surface of the M_3 and M_4-coated samples was very uniform, indicating that the nanoparticle was uniformly covered in the fabric surface.

3.7. UPF measurement

The ultraviolet protection factor (UPF) measurements were made using a Jasco V-670 spectrophotometer to determine the transmittance of the UV radiation in the conditioned samples, thus evaluating its UV protection properties. The UV-blocking results of uncoated cotton, ppy, M_1, M_2, M_3 and M_4 coated cotton fabrics are shown in Fig. 9(a–f), and the values are given in Table 2. Ultraviolet protection factor (UPF) was computed using Table 2.

$$\text{UPF} = \frac{\sum_{280 \text{ nm}}^{400 \text{ nm}} E_\lambda S_\lambda \Delta_\lambda}{\sum_{280 \text{ nm}}^{400 \text{ nm}} E_\lambda S_\lambda T_\lambda \Delta_\lambda}$$
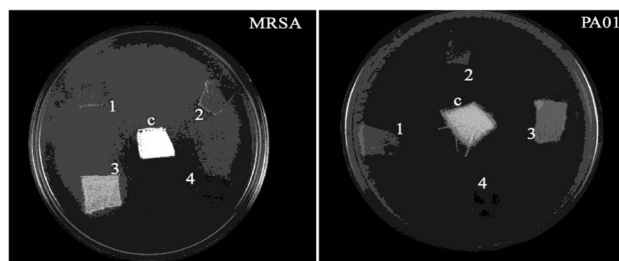

Fig. 11 Antibacterial activity of the negative control (c) DMSO, (1) M_1 coated, (2) M_2 coated, (3) M_3 coated, and (4) M_4 coated cotton.

Table 4 Physical properties of the fabrics

| Specimen | Absorbency (seconds) | Tensile strength (lbf) | | Tearing strength (lbf) | | CRA (W + F) |
		Warp	Weft	Warp	Weft	
Uncoated	6	53.5	42.5	2.8	2.2	120
M_1	8	56.5	49.4	2.4	2.1	116
M_2	9	55.1	48.7	2.5	2.1	128
M_3	10	56.5	49.2	2.7	2.2	134
M_4	11	64.5	40.2	2.8	2.3	141

Table 5 Flame retardancy

Test fabric	Flame retardant (concentration)	Coating method	Char length (cm)	Ref.
Cotton	Ammonium aluminum sulphate dodecahydrate (0.2 M)	Pad-dry-cure	0.2	63
Cotton	Diethyl-4-methylpiperazin-1-yl phosphoramidate (3.64 ml)	Dip coating	2.3	64
Cotton	BTCA–CA–MF ($70 : 70 : 65$ g L^{-1})	Pad-dry-cure	4.1	65
Wool	$ZrOCl_2$–citric acid–formic acid ($7.95 : 9.5 : 8.0\%$)	Dip coating	0.85	66
Silk	Dimethyl-l-2-(methacryloyloxyethyl)phosphate (20%)	Dip coating	4.5	67
Cotton/polyester	BTCA–uccinic acid–ZnO ($0.5 : 0.5 : 0.25\%$)	Pad-dry-cure	0.30	68
Cotton	Ppy–MgO–CNT (12.5 g $: 1.0$ g $: 0.33$ ml $: 1.0$ g)	pad-dry-cure	**0.3**	**Our work**

where S_λ is the spectral irradiation in the UV region (280–400 nm); E_λ is the relative erythemal spectral effectiveness, T_λ is the spectral transmittance of the fabric; Δ_λ is the increment relating to the wavelength, and λ is the wavelength in nanometer.

In the samples, M_1, M_2, M_3, and M_4, the reflectance values decreased, confirming the presence of UV blocking material (MgO nanoparticles). In coated ppy, the lowest reflectance is observed in the 200–385 nm region. This may be due to the higher possibility of contact between the UV wavelengths without the presence of polycarboxylic acid molecules.[62]

3.8. Antibacterial activity

Agar diffusion assay. The zone of inhibition was observed for all of the test samples against MRSA and PAO1 bacteria. Uncoated cotton fabric containing DMSO served as the control (c). Among these, the MPN powder exhibited the maximum zone of inhibition (Fig. 10).

The zone of inhibition was observed for all coated test samples against MRSA and PAO1 bacteria, when the uncoated cotton fabric containing DMSO is served as the control (c) (Fig. 11). In the meantime, the zone of inhibition data is given in Table 3.

The results indicate that the coated fabric did not show a good zone of inhibition. The agar diffusion method result

Table 6 Ultraviolet protection

Test fabric	UV blocking agent (concentration)	Coating method	UPF	Ref.
Cotton	Copper acetate (0.5 M)	Pad-dry-cure	42.0	69
Cotton	Titania nanosols (45 ml)	Sol–gel process and pad-dry- cure	47.0	70
Cotton	Polyurethane–ZnO ($15 : 1$ wt%)	Electrospinning	50	71
Cotton	Titania-silica nanosol (6 ml)	Dip-dry-cure	73	72
Cotton	PU–nano-TiO_2 (15 g $L^{-1} : 0.1$ wt%)	Layer-by-layer deposition	50	73
Cotton	Chitosan–TiO_2 (4% w/v $: 1$ g)	Pad-dry-cure	50	74
Cotton	TiO_2 nanoparticles (3 wt%)	Linking agent anchoring	50	75
Cotton	Needle-shaped ZnO nanorod (0.001 M)	*In situ* growth	105.1	76
Cotton	CA–SHP–nano-TiO_2 ($50 : 25 : 5$ g L^{-1})	pad-dry-cure	135.9	77
Cotton	PU–MWNT ($2.5 : 15$ wt%)	Pad-dry-cure	421.0	78
Cotton	Chitosan–graphene ($2 : 1.0$ wt%)	Pad-dry-cure	465.8	73
Cotton	Dumbbell-shaped ZnO crystallites (0.01 M)	Low-temperature growth and hydrothermal	800	75
Wool	$CuSO_4$ (10 ml L^{-1})	Dyeing process	65.0	74
Polyester	Silk sericin (5 ml)	Pad-dry-cure	30.9	75
Polyester	Alginates and nano-TiO_2 ($0.1\% : 0.1$ M)	Dip-dry-cure	119.8	79
Polyester	Nano structured silver (72.55 wt%)	Magnetron sputtering	302.1	80
Nylon	ZnO–PMMA nanocomposites (1 g $: 5$ wt%)	Pad-dry-cure	19.4	81
Cotton	Ppy–MgO–CNT (12.5 g $: 1.0$ g $: 0.33$ ml $: 1.0$ g)	Pad-dry-cure	**30**	**Our work**

Table 7 Antibacterial activity

Test fabric	Antibacterial agent (concentration)	Coating method	Zone of inhibition (mm)		
			S. aureus	*E. coli*	Ref.
Cotton	Ag-NPs colloidal solution (100 ppm)	Dip coating	0.5	1.0	82
Cotton	5,5-Dimethylhydantoin (32 g)	Plasma and pad-dry-cure	1.36	0	83
Cotton	ZnO–ureolytic (0.02 M : 1 g L^{-1})	Dip coating	1.6	2.0	84
Cotton	Ag–polyvinyl pyrrolidone colloid (50 µg ml^{-1} : 240 ppm)	Dip coating	12	11	85
Cotton	*Punica granatum* L. and *Terminalia chebula* plant extract (10 g)	Pad-dry-cure	30	28	86
Cotton	Poly-*N*-vinyl-2-pyrrolidone–ZnO (2% : 20 mg L^{-1})	Pad-dry-cure	38	47	87
Polyester	Al_2O_3–Ag–TiO_2 (1 : 1 g)	Pad-dry-cure	12	11	88
Cotton/polyester	Triclosan and Siligen (15 : 3%)	Pad-dry-cure	47	38	89
Cotton	Ppy–MgO–CNT (3 : 0.2 : 0.8 g)	Pad-dry-cure	**4.0**	**3.0**	**Our work**

reveals that M_4 exhibited the maximum zone of inhibition against the test pathogens.

3.9. Physical properties of the fabrics

Water absorbency of the coated fabric was compared to that of uncoated fabrics. The absorbency was superior for the fabrics coated with M_3 and M_4 composite. The tensile strength of the M_4 coated fabric with catalyst has shown enhanced performance compared to the others (Table 4). This may be due to the intermolecular and intramolecular crosslinking, which reduces the possibility of getting even the stress distribution, causing reduction in the capacity to resist shipment. The tearing strength of sample M_4 has shown improved performance compared to the uncoated one. This may be due to the crosslinking ability of BTCA, hindered by the presence of hydroxyl groups in the structure. The sample coated with the composite showed a moderate increase in the crease recovery angle (CRA) values. The CRA angle of the composite sample M_4 reached up to 140°. This shows that the crosslinking affected by the esterification reaction of the coated cotton has imparted better crease recovery behavior. This may be because BTCA has one more carboxylic acid group, which bonds to the adjacent carbons in their molecular backbones.

4. Comparative study

Cotton fabrics coated with composites prepared from carboxylic acids and catalysts with metal oxide were evaluated for flame retardancy (Table 5), UPF and antibacterial applications. BTCA with SHP effectively increased the char formation. The nanoparticles deposited on the fabric surface showed stability both before and after washing, which was confirmed through SEM-EDAX analysis. The flammability of the M_4 coated fabric was found to be 0.3 cm better than that of the uncoated fabric. The UPF value of the M_4 coated fabric is 30, which suggests that the ppy–MgO–CNT coated cotton fabrics is a promising multifunctional textile material for military and UPF protection and antibacterial applications (Tables 6 and 7).

Conflicts of interest

There are no conflicts to declare.

Acknowledgements

References

1 A. Ashori, Y. Hamzeh and F. Amani, Chemical composition and fibre morphology, *J. Polym. Environ.*, 2011, **19**, 297–300.

2 A. Ashori, M. Ornelas, S. Sheshmani and N. Cordeiro, Influence of mild alkaline treatment on the cellulosic surfaces active sites, *Carbohydr. Polym.*, 2012, **88**, 1293–1298.

3 S. Cassaignon, M. Koelsch and J. P. Jolivet, Selective Synthesis of Brookite, Anatase and Rutile Nanoparticles: Thermolysis of $TiCl_4$ in Aqueous Nitric Acid, *J. Mater. Sci.*, 2007, **42**, 6689–6695.

4 N. Cordeiro, M. Ornelas, A. Ashori, S. Sheshmani and H. Norouzi, Investigation on the surface properties of chemically modified natural fibres using inverse gas chromatography, *Carbohydr. Polym.*, 2012, **87**, 2367–2375.

5 N. R. Dhineshbabu, P. Manivasakan, A. Karthik and V. Rajendran, Hydrophobicity, flame retardancy and antibacterial properties of cotton fabrics functionalised with MgO/methyl silicate nanocomposites, *RSC Adv.*, 2014, **4**, 32162–32173.

6 Z. Ding, X. Hu, P. L. Yue, G. Q. Lu and P. F. Greenfield, Synthesis of anatase TiO_2 supported on porous solids by chemical vapor deposition, *Catal. Today*, 2001, **68**, 173–182.

7 W. A. Esmail, A. M. Y. Darwish, O. A. Ibrahim and M. F. Abadir, The Effect of Magnesium Chloride Hydrate on the Fire Retardation of Cellulosic Fibers, *J. Therm. Anal. Calorim.*, 2001, **63**, 831–838.

8 H. Feng, B. Wang, L. Tan, N. Chen and N. Wang, ChenB. Polypyrrole/hexadecylpyridinium chloride-modified graphite oxide composites: Fabrication, characterization, and application in supercapacitors, *J. Power Sources*, 2014, **246**, 621–628.

9 D. D. Gagliardi and F. B. Shippee, Epoxy Resin Blended Finishes for White Cottons, *Text. Res.*, J1959, **29**, 54–65.

10 M. P. Gashti and A. Elahi, UV radiation inducing succinic acid/silica-kaolinite network on cellulose fiber to improve the functionality, *Composites, Part B*, 2013, **48**, 158–166.

11 J. Y. Gong, W. H. Pu, C. Z. Yang and J. L. Zhang, Novel one-step preparation of tungsten loaded TiO_2 nanotube arrays with enhanced photoelectrocatalytic activity for pollutant degradation and hydrogen production, *Catal. Commun.*, 2013, **36**, 89–93.

12 H. Gui, X. Zhang, Y. Lin, W. Dong, Q. Wang, J. Gao, Z. Song, J. Lai and J. Qiao, Effect of dispersion of nano-magnesium hydroxide on the flammability of flame retardant ternary composites, *Compos. Sci. Technol.*, 2007, **67**, 974–980.

13 P. J. Hauser, C. B. Smith and M. M. Hashem, Ionic Crosslinking Of Cotton, *Autex Res. J.*, 2004, **4**, 95–100.

14 A. Hebeish, M. Hashem, A. Abdel-Rahman and Z. H. El-Hilw, Improving easy care nonformaldehyde finishing performance using polycarboxylic acids *via* precationization of cotton fabric, *J. Appl. Polym. Sci.*, 2006, **100**, 2697–2704.

15 S. Hsieh, F. R. Zhang and H. Sili, Anti-ultraviolet and physical properties of woolen fabrics cured with citric acid and TiO_2/chitosan, *J. Appl. Polym. Sci.*, 2006, **100**, 4311–4319.

16 K. Y. Jung and S. B. Park, Anatase-phase titania: preparation by embedding silica and photocatalytic activity for the decomposition of trichloroethylene, *J. Photochem. Photobiol., A*, 1999, **127**, 117–122.

17 J. W. Kim, F. Liu, H. J. Choi, S. H. Hong and J. Joo, Intercalated polypyrrole/Na$^+$-montmorillonite nanocomposite *via* an inverted emulsion pathway method, *Polymer*, 2003, **44**, 289–293.

18 Q. Kong and H. Qian, Low-temperature synthesis of $Mg(OH)_2$ nanoparticles from MgO as halogen-free flame retardant for polypropylene, *Fire Mater.*, 2014, **38**, 145–154.

19 K. Krishnamoorthy, J. Y. Moon, H. B. Hyun, S. K. Cho and S. J. Kim, Mechanistic investigation on the toxicity of MgO nanoparticles toward cancer cells, *J. Mater. Chem.*, 2012, **22**, 24610–24617.

20 D. Kumar, V. B. Reddy, B. G. Mishra, R. K. Rana, M. N. Nadagouda and R. S. Varma, Nanosized magnesium oxide as catalyst for the rapid and green synthesis of substituted 2-amino-2-chromenes, *Tetrahendran*, 2007, **63**, 3093–3097.

21 E. S. Lee and H. J. Kim, Durable press finish of cotton/polyester fabrics with 1,2,3,4 butanetetracarboxylic acid and sodium propionate, *J. Appl. Polym. Sci.*, 2001, **81**, 654–661.

22 J. M. Cardamone and J. G. Phillips, Enzyme-mediated Crosslinking of Wool. Part II: Keratin and Transglutaminase, *Text. Res. J.*, 2007, **77**, 227–283.

23 C. H. Lu, W. H. Wu and R. B. Kale, Microemulsion-mediated hydrothermal synthesis of photocatalytic TiO_2 powders, *J. Hazard. Mater.*, 2008, **154**, 649–654.

24 A. Menard, D. Drobne and A. Jemec, Ecotoxicity of nanosized TiO_2. Review of *in vivo* data, *Environ. Pollut.*, 2011, **159**, 677–684.

25 K. Sanders, L. L. Degn and W. R. Mundy, In vitro phototoxicity and hazard identification of nano-scale titanium dioxide, *Toxicol. Appl. Pharmacol.*, 2012, **258**, 226–236.

26 J. J. Yin, J. Liu and M. Ehrenshaft, Phototoxicity of nano titanium dioxides in HaCaT keratinocytes-generation of reactive oxygen species and cell damage, *Toxicol. Appl. Pharmacol.*, 2012, **263**, 81–88.

27 I. L. Hsiao and Y. J. Huang, Effects of various physicochemical characteristics on the toxicities of ZnO and TiO_2 nanoparticles toward human lung epithelial cells, *Sci. Total Environ.*, 2011, **409**, 1219–1228.

28 Y. Lu and C. Q. Yang, Fabric Yellowing Caused by Citric Acid as a Crosslinking Agent for Cotton, *Text. Res. J.*, 1990, **69**, 685–690.

29 L. Maedler, H. K. Kammler, R. Mueller and S. E. Pratsinis, Controlled synthesis of nanostructured particles by flame spray pyrolysis, *J. Aerosol Sci.*, 2002, **33**, 369–389.

30 M. A. Chougule, S. G. Pawar, P. R. Godse, R. N. Mulik, S. Sen and V. B. Patil, Synthesis and Characterization of Polypyrrole (PPy) Thin Films, *Soft Nanosci. Lett.*, 2011, **1**, 6–10.

31 Z. Mao and C. Q. Yang, IR spectroscopy study of cyclic anhydride as intermediate for ester crosslinking of cotton cellulose by polycarboxylic acids. V. Comparison of 1,2,4-butanetricarboxylic acid and 1,2,3-propanetricarboxylic acid, *J. Appl. Polym. Sci.*, 2001, **81**, 2142–2150.

32 R. Mehran, K. Majid and N. Behzad, Synthesis of high surface area nanocrystalline MgO by pluronic P123 triblock copolymer surfactant, *Powder Technol.*, 2011, **205**, 112–116.

33 H. Minami, K. Kinoshita, T. Tsuji and H. Yanagimoto, Preparation of Highly Crystalline Magnesium Oxide and Polystyrene/Magnesium Hydroxide Composite Particles by Sol-Gel Processes in an Ionic Liquid, *J. Phys. Chem. C*, 2012, **116**, 14568–14574.

34 S. T. Navale, G. D. Khuspe, M. A. Chougule and V. B. Patil, Room temperature NO_2 gas sensor based on PPy/α-Fe_2O_3 hybrid nanocomposites, *Ceram. Int.*, 2014, **40**, 8013–8020.

35 A. Nazari, M. Montazer, A. Rashidi, M. Yazdanshenas and M. Anary-Abbasinejad, Nano TiO_2 photo-catalyst and sodium hypophosphite for cross-linking cotton with poly carboxylic acids under UV and high temperature, *Appl. Catal., A*, 2009, **371**, 10–16.

36 B. Ozturk, T. Batar and B. Tufan, Production of MgO Catalyzor Nanoparticles by Flame Spray Pyrolysis Method, *Journal of Ore Dressing*, 2012, **28**, 14–18.

37 H. C. Pant, M. K. Patra, S. C. Negi, A. Bhatia, S. R. Vadera and N. Kumar, Studies on conductivity and dielectric properties

of polyaniline-zinc sulphide composites, *Bull. Mater. Sci.*, 2006, **29**, 379–384.

38 J. K. Patra and S. Gouda, Application of nanotechnology in textile engineering: an overview, *J. Eng. Technol. Res.*, 2013, **5**, 104–111.

39 V. Rajendran, N. R. Dhineshbabu, R. Rajesh Kanna and K. V. Kaler, Enhancement of thermal stability, flame retardancy, and antimicrobial properties of cotton fabrics functionalized by inorganic nanocomposites, *Ind. Eng. Chem. Res.*, 2014, **53**, 19512–19524.

40 O. Sauperl, K. B. Stana-Kleinschek, M. Voncina, S. Sfiligoj and A. Majcen-Le Marechal, Application of Spectrophotometric Methods in Assessing the Influence of Alkaline Treatment on the Degree of Crosslinking of Cotton Cellulose with BTCA, *Croat. Chem. Acta*, 2003, **76**, 293–298.

41 M. Selvaraj, S. Palraj, K. Maruthan, G. Rajagopal and G. Venkatachari, Polypyrrole as a protective pigment in organic coatings, *Synth. Met.*, 2008, **158**, 888–899.

42 H. Shao, J. Y. Sun and W. D. Meng, Water and Oil Repellent and Durable Press Finishes for Cotton Based on a Perfluoroalkyl-Containing Multi-Epoxy Compound and Citric Acid, *Text. Res. J.*, 2004, **74**, 851–855.

43 B. Sharia Zadeh and O. Moradi, Surface functionalization of multiwalled carbon nanotubes with chitosan and magnesium oxide nanoparticles by microwave-assisted synthesis, *Polym. Compos.*, 2014, **10**, 20–50.

44 S. Shekarriz and Z. Shariatinia, Effect of Fluorination Treatment on Cotton Wettability, Dyeability and Mechanical Properties and Characterization of Surface Changes by XPS, *Prog. Color, Color. Coat.*, 2014, **7**, 85–93.

45 W. Sricharussin, W. Ryo-Aree, W. Intasen and S. Poungraksakirt, Effect of Boric Acid and BTCA on Tensile Strength Loss of Finished Cotton Fabrics, *Text. Res. J.*, 2004, **74**, 475–480.

46 R. Strobel and S. E. Pratsinis, Flame aerosol synthesis of smart nanostructured materials, *J. Mater. Chem.*, 2007, **17**, 4743–4756.

47 S. Suresh and D. Arivuoli, Synthesis and characterization of Pb$^+$ doped MgO nanocrystalline particles, *Dig. J. Nanomater. Biostructures*, 2011, **6**, 1597–1603.

48 G. Tillet, B. Boutevin and B. Ameduri, Chemical reactions of polymer crosslinking and post-crosslinking at room and medium temperature, *Prog. Polym. Sci.*, 2011, **36**, 191–217.

49 D. TobinggS and K. Andrew, Molecular parameters and their relation to the adhesive performance of emulsion acrylic pressure-sensitive adhesives. II. Effect of crosslinking, *J. Appl. Polym. Sci.*, 2001, **79**, 2558–2564.

50 F. Taleshi and A. A. Hosseini, Synthesis of uniform MgO/CNT nanorods by precipitation method, *J. Nanostruct. Chem.*, 2012, **3**, 1–5.

51 M. J. Uddin, F. Cesano, F. Bonino, S. Bordiga, G. Spoto, D. Scarano and A. Zecchina, Photoactive TiO$_2$ films on cellulose fibres: synthesis and characterization, *J. Photochem. Photobiol., A*, 2007, **189**, 286–294.

52 H. Wang, Y. Wu and B. Q. Xu, Preparation and characterization of nanosized anatase TiO$_2$ cuboids for photocatalysis, *Appl. Catal., B*, 2005, **59**, 139–146.

53 S. S. Watson, D. Beydoun and J. A. Scott, Amal.The effect of preparation method on the photoactivity of crystalline titanium dioxide particles, *Chem. Eng. J.*, 2003, **95**, 213–220.

54 C. M. Welch, Tetracarboxylic Acids as Formaldehyde-Free Durable Press Finishing Agents: Part I: Catalyst, Additive, and Durability Studies1, *Text. Res. J.*, 1988, **58**, 480–486.

55 C. H. Xue, W. Yin, S. T. Jia and J. Z. Ma, UV-durable superhydrophobic textiles with UV-shielding properties by coating fibers with ZnO/SiO$_2$ core/shell particles, *Nanotechn*, 2011, **22**, 415–603.

56 C. Q. Yang, FT-IR Spectroscopy Study of the Ester Crosslinking Mechanism of Cotton Cellulose, *Text. Res. J.*, 1991, **61**, 433–494.

57 C. Q. Yang, X. Wang and I. Jang, Nonformaldehyde Durable Press Finishing of Cotton Fabrics by Combining Citric Acid with Polymers of Maleic Acid, *Text. Res. J.*, 1998, **68**, 457–464.

58 C. Q. Yang, X. Wang and I. S. Kang, Ester Crosslinking of Cotton Fabric by Polymeric Carboxylic Acids and Citric Acid, *Text. Res. J.*, 1997, **67**, 334–342.

59 C. Q. Yang and X. Wang, Formation of Cyclic Anhydride Intermediates and Esterification of Cotton Cellulose by Multifunctional Carboxylic Acids: An Infrared Spectroscopy Study, *Text. Res. J.*, 1996, **66**, 595–603.

60 K. B. Yazhini and H. G. Prabu, Antibacterial Activity of Cotton Coated With ZnO and ZnO-CNT Composites, *Appl. Biochem. Biotechnol.*, 2015, **175**, 93–102.

61 Z. Qiaoran, Z. Li, X. Li, L. Yu, Z. Zhang and Z. Wu, Zinc ferrite nanoparticle decorated boron nitride nanosheet: preparation, magnetic field arrangement, and flame retardancy, *Chem. Eng. J.*, 2019, **356**, 680–692.

62 L. Yua, K. Deana and L. Li, Polymer blends and composites from renewable resources, *Prog. Polym. Sci.*, 2006, **31**, 576–602.

63 A. Edwin sundar and G. Nalankilli, Polyfunctional finishes on Cotton Textiles, *Indian J. Fibre Text. Res.*, 2012, **37**, 364–371.

64 L. L. Zhang, S. Y. Zhao, X. N. Tian and X. S. Zhao, Layered Graphene Oxide Nanostructures with Sandwiched Conducting Polymers as Supercapacitor Electrodes, *Langmuir*, 2010, **26**, 17624–17628.

65 S. M. Mostashari and S. Z. Mostashari, Thermogravimetry of Deposited Ammonium Aluminum Sulfate Dodecahydrate used as Flame-Retardant for cotton Fabrics, *Cellul. Chem. Technol.*, 2009, **43**, 455–460.

66 D. Thach-Mien Nguyen, S. C. Chang, B. Condon, M. Uchimiya and C. Fortier, Development of an environmentally friendly halogen-free phosphorus–nitrogen bond flame retardant for cotton fabrics, *Polym. Adv. Technol.*, 2012, **23**, 1555–1563.

67 D. Katovic, S. B. Vukusic, S. F. Grgac, B. Lozoand and D. Banic, Flame retardancy of paper obtained with environmentally friendly agents, *Fibres Text. East. Eur.*, 2009, **17**, 90–94.

68 M. B. Moghadam, A Comparative Optimization Study of Flame Retardancy of Wool Fabric with and Without Robust Parameter Design Approach, *World Appl. Sci. J.*, 2011, **13**, 1430–1435.

69 J. Guan, H. Lu and Y. Chen, Apparel Performance of Flame Retardant Silk Fabrics, *J. Eng. Fibers Fabr.*, 2013, **8**, 30–35.

70 M. M. Abd El-Hady, A. Farouk and S. Sharaf, Flame retardancy and UV protection of cotton based fabrics using nano ZnO and polycarboxylic acids, *Carbohydr. Polym.*, 2013, **92**, 400–406.

71 R. H. Wang, J. H. Xin and X. M. Tao, UV-Blocking Property of Dumbbell-Shaped ZnO Crystallites on Cotton Fabrics, *Inorg. Chem.*, 2005, **44**, 3926–3930.

72 Z. Mao, Q. Shi, L. Zhang and H. Cao, The formation and UV-blocking property of needle-shaped ZnO nanorod on cotton fabric, *Thin Solid Films*, 2009, **517**, 2681–2686.

73 N. A. Ibrahim, R. Refaie and A. F. Ahmed, Novel approach for attaining cotton fabric with multi-functional properties, *J. Ind. Text.*, 2010, **40**, 65–83.

74 S. Mondal and J. L. Hu, A novel approach to excellent UV protecting cotton fabric with functionalized MWNT containing water vapor permeable PU coating, *J. Appl. Polym. Sci.*, 2007, **103**, 3370–3376.

75 M. Tian, X. Tang, L. Qu, S. Zhu, X. Guo and G. Han, Robust ultraviolet blocking cotton fabric modified with chitosan/graphene nanocomposites, *Mater. Lett.*, 2015, **15**, 340–343.

76 R. Mongkholrattanasit, J. Krystufek, J. Wiener and M. Vikova, Dyeing, Fastness, and UV Protection Properties of Silk and Wool Fabrics Dyed with Eucalyptus Leaf Extract by the Exhaustion Process, *Fibres Text. East. Eur.*, 2011, **19**, 94–99.

77 M. L. Gulrajani, K. P. Brahma, P. S. Kumar and R. Purwar, Application of silk sericin to polyester fabric, *J. Appl. Polym. Sci.*, 2008, **109**, 314–321.

78 D. Mihailovic, Z. Saponjic, M. Radoicic, T. Radetic, P. Jovancic and J. Nedeljkovic, Functionalization of polyester fabrics with alginates and TiO$_2$ nanoparticles, *Carbohydr. Polym.*, 2010, **79**, 526–532.

79 S. X. Jiang, W. F. Qin, R. H. Guo and L. Zhang, Surface functionalization of nanostructured silver-coated polyester fabric by magnetron sputtering, *Surf. Coat. Technol.*, 2010, **204**, 3662–3667.

80 V. SornaGowri, L. Almeida, M. T. P. DeAmorim, N. C. Pacheco, A. P. Souto and M. F. Esteves, Functional finishing of polyamide fabrics using ZnO–PMMA nanocomposites, *J. Mater. Sci.*, 2010, **45**, 2427–2435.

81 M. L. Gulrajani, K. P. Brahma, P. S. Kumar and R. Purwar, Application of silk sericin to polyester fabric, *J. Appl. Polym. Sci.*, 2008, **109**, 314–321.

82 M. H. E. Rafie, H. B. Ahmed and M. K. Zahran, Characterization of nanosilver coated cotton fabrics and evaluation of its antibacterial efficacy, *Carbohydr. Polym.*, 2014, **107**, 174–181.

83 C. E. Zhou and C. W. Kan, Plasma-enhanced regenerable 5,5-dimethylhydantoin (DMH) antibacterial finishing for cotton fabric, *Appl. Surf. Sci.*, 2015, **328**, 410–417.

84 P. Dhandapani, A. S. Siddarth, S. Kamalasekaran, S. Maruthamuthu and G. Rajagopal, Bio-approach: Ureolytic bacteria mediated synthesis of ZnO nanocrystals on cotton fabric and evaluation of their antibacterial properties, *Carbohydr. Polym.*, 2014, **103**, 448–455.

85 S. Ghosh, A. Upadhay, A. K. R. Singh and A. Kumar, Investigation of antimicrobial activity of nano particle loaded cotton fabrics which may promote wound healing, *Int. J. Pharma Bio Sci.*, 2010, **1**, 1–10.

86 R. Rathinamoorthy, S. Udayakumar and G. Thilagavathi, Antibacterial Efficacy Analysis of Punica Granatum L. Leaf, Rind And Terminalia Chebula Fruit Extract Treated Cotton Fabric Against Five Most Common Human Pathogenic Bacteria, *Int. J. Pharm. Life Sci.*, 2011, **10**, 1147–1153.

87 S. Selvam and M. Sundrarajan, Functionalization of cotton fabric with PVP/ZnO nanoparticles for improved reactive dyeability and antibacterial activity, *Carbohydr. Polym.*, 2012, **87**, 1419–1424.

88 W. M. Raslan, U. S. Rashed, H. E. Sayad and A. A. E. Halwagy, Ultraviolet protection, flame retardancy and antibacterial properties of treated polyester fabric using plasma-nano technology, *Mater. Sci. Appl.*, 2011, **2**, 1432–1442.

89 N. A. Ibrahim, M. Hashem, W. A. E. Sayed, S. E. Husseiny and E. E. Enany, Enhancing antimicrobial properties of dyed and finished cotton/polyester fabrics, *AATCC Rev.*, 2010, **9**, 56–64.